Journal of the Korean Electrochemical Society
Vol. 5, No. 2, 2002, 86-92

총 설

Application of Monte Carlo Simulation to Intercalation Electrochemistry II. Kinetic Approach to Lithium Intercalation into $LiMn_2O_4$ Electrode

Sung-Woo Kim and Su-Il Pyun†

Corrosion and Interfacial Electrochemistry Research Laboratory at Department of Materials Science and Engineering Korea Advanced Institute of Science and Technology 373-1 Guseong-dong, Yuseong-gu, Daejeon 305-701, Republic of Korea
(Received January 11, 2002 : Accepted May 8, 2002)

Abstract. The present article is concerned with the application of the kinetic Monte Carlo simulation to electrochemistry of lithium intercalation from the kinetic view point. Basic concepts of the kinetic Monte Carlo method and the transition state theory were first introduced, and then the simulation procedures were explained to evaluate diffusion process. Finally the kinetic Monte Carlo method based upon the transition state theory was employed under the cell-impedance-controlled constraint to analyse the current transient and the linear sweep voltammogram for the $LiMn_2O_4$ electrode, one of the intercalation compounds. From the results, it was found that the kinetic Monte Carlo method is much relevant to investigate kinetics of the lithium intercalation in the field of electrochemistry.

초 록 : 속도론적 관점에서 키네틱 몬테 카를로 방법의 전기화학적 리튬 인터칼레이션에로의 응용에 대하여 다루었다. 우선 키네틱 몬테 카를로 방법과 전이상태이론의 기본 개념을 소개하였고, 확산거동을 평가하기 위한 시뮬레이션 과정을 설명하였다. 마지막으로 인터칼레이션 화합물중 $LiMn_2O_4$ 전극에 대해 전류 추이곡선과 선형 포텐셜 전류곡선을 해석하기 위해서 전이상태이론에 근거한 키네틱 몬테 카를로 방법을 셀-저항 제어조건하에서 사용하였다. 이로부터 키네틱 몬테 카를로 방법이 전기화학분야에서 리튬 인터칼레이션의 속도론적 연구에 매우 유용함을 알 수 있었다.

Key words : Cell-impedance-controlled constraint, Kinetic Monte Carlo simulation, $LiMn_2O_4$ electrode, Lithium Intercalation, Transition state theory

1. Introduction

With the advent of fast computers, the Monte Carlo simulation has become the popular method to analyse the thermodynamic properties of a system at an equilibrium state. However, the classical Monte Carlo method is not well suited to explain the behaviour of the system over time. Instead, the kinetic Monte Carlo method (KMC), so-called dynamic Monte Carlo method has been employed to investigate non-equilibrium or relaxation process of a number of such interesting physical phenomena as chemical reaction,[1-3] adsorption or deposition,[4] and diffusion of adsorbates[5-8] on surface of solids. In the kinetic Monte Carlo method, the behaviour of the systems over time can be explained in terms of the rates of those reactions.

In the kinetic Monte Carlo method, the thermally activated, stochastic hopping process is well described according to the transition state theory (TST).[5-9] Recently, the kinetic Monte Carlo method based upon the lattice gas model has been employed in the field of electrochemistry to analyse diffusion of ions on the electrode surface or in the bulk electrode, especially diffusion of lithium ions intercalated into transition metal oxides.[9,10] In those works, the kinetic properties such as the chemical and component diffusion coefficients of lithium ions in the transition metal oxides have been successfully investigated by using the kinetic Monte Carlo methods with the transition state theory. Since the lithium intercalation consists of multiple thermally activated processes such as migration or diffusion of lithium ions in the electrolyte, interfacial reaction at the electrode surface, and diffusion of lithium ions in the bulk electrode, the kinetic Monte Carlo study gives a better understanding of kinetics of the lithium intercalation.

This article reviewed the kinetic Monte Carlo method based upon the transition state theory to analyse electrochemical lithium intercalation from the kinetic view point. First this article introduced fundamentals of the kinetic Monte Carlo method and the transition state theory, and then explained the Monte Carlo procedures to evaluate diffusion process. Finally, the kinetic Monte Carlo method with appropriate algorithms was proposed to analyse the current responses during the potential step and scan. In this article, we presented the results theoretically calculated for the $LiMn_2O_4$ electrode, one of the well-known intercalation compounds.

2. Fundamentals of Kinetic Monte Carlo Method

2.1. Kinetic Monte Carlo method

The kinetic Monte Carlo method is well suited to study kinetics of the system near equilibrium as well as far from equilibrium. In the kinetic Monte Carlo method, a configura-

†E-mail: sipyun@mail.kaist.ac.kr

tion of the system is generated by a stochastic process using a transition probability which satisfies a mass balance condition[11)]

$$W_{tr}(\{c\}\rightarrow\{c'\})P(\{c\},t) = W_{tr}(\{c'\}\rightarrow\{c\})P(\{c'\},t) \quad (1)$$

where $\{c\}$ and $\{c'\}$ are a sequence of the configurations of the system generated one after the other from the previous configuration of the system, corresponding to a set of the local occupation number of sites, *i.e.* $\{c\} = \{c_1, c_2 \ldots, c_i \ldots\}$; $W_{tr}(\{c\}\rightarrow\{c'\})$ and $W_{tr}(\{c'\}\rightarrow\{c\})$, the transition probabilities from the configuration of the system $\{c\}$ to $\{c'\}$ and $\{c'\}$ to $\{c\}$, respectively, and $P(\{c\}, t)$ and $P(\{c'\}, t)$ represent the probabilities that the configurations of the system $\{c\}$ and $\{c'\}$, respectively, occur at t Monte Carlo step (MCS) time.

The master equation that describes how the configuration of the system $\{c\}$ evolves with time is expressed as[11,12)]

$$\frac{\partial P(\{c\},t)}{\partial t} = \sum [W_{tr}(\{c'\}\rightarrow\{c\})P(\{c'\},t) - W_{tr}(\{c\}\rightarrow\{c'\})P(\{c\},t)] \quad (2)$$

Since the change in the configuration of the system involves a number of trial jumps of atoms or ions from one site to the empty nearest neighbor sites, it is then convenient to introduce the flux of atoms or ions per unit jump length,

$$\frac{\partial P(\{c\},t)}{\partial t} = -\sum j(\{c\},t) = -J(\{c\},t) \quad (3)$$

where $J(\{c\}, t)$ is total flux of atoms or ions per unit jump length in the lattice with the configuration of the system $\{c\}$ at t MCS time. Eq. (3) is nothing but the discrete expression of the Fick's diffusion equation.

2.2. Transition state theory

In Eqs. (1) and (2), the transition probability W_{tr} is determined based upon the transition state theory. The transition state theory or the activated complex theory is a classical model of the thermally activated processes on a microscopic scale in which atoms or ions jump over an energy barrier larger than k_BT.[13)] In the theory, the rates of the thermally activated processes are equal to the number of activated complexes passing over the energy barrier per unit time. Therefore, W_{tr} is interpreted as a microscopic analog of the rate constant k,

$$W_{tr} = w^0 \exp(-E_a/k_BT) = k \quad (4)$$

where w^0 is the effective jump frequency of atoms or ions; E_a, the activation energy; k_B, the Boltzmann's constant, and T represents the absolute temperature.

The activation energy E_a in Eq. (4) of the thermally activated process is determined based upon the lattice gas model. In the lattice gas model, the total energy of the lattice H in the presence of a chemical potential μ is simply written as

$$H = J\sum_{ij} c_i c_j - \mu \sum_{i=1}^{N} c_i \quad (5)$$

where c_i is the occupation number of the site i: if the site i is occupied by an atom or ion, $c_i = 1$; otherwise, $c_i = 0$. A particular configuration of the lattice is specified by the set of variables $\{c_1, c_2 \ldots, c_i, c_j \ldots, c_N\}$ for all the sites of the lattice. In Eq. (5), the first summation corresponds to the interaction energy E_{int}, where the positive value of J means the repulsive interaction between atoms or ions, while the negative value of J indicates the attractive interaction.

Let us first consider the transition state theory generally used for diffusion process on the surface of solids. In the case of the surface diffusion of adsorbates, μ is constant within the whole electrode during diffusion process. In this case, Uebing *et al.*[5-8)] proposed that the potential energy of the transition state is invariant with concentration of adsorbates, and hence the activation energy for diffusion is simply given by

$$E_a = E_{tran} - E_{ini} = E_a^0 - \Delta E_{int} \quad (6)$$

where E_{tran} and E_{ini} are the potential energy of the transition and the initial states, respectively; E_a^0, the activation energy in case there is no interactions between atoms or ions, and ΔE_{int} represents the interaction energy change. In Eq. (6), $\Delta E_{int} > 0$ for the repulsive interaction which decreases the activation energy, while $\Delta E_{int} < 0$ for the attractive interaction which increases the activation energy. It should be noted that the activation energy E_a increases or decreases by the amount of the interaction energy change ΔE_{int} in Eq. (6).

On the other hand, in the case of the interfacial reaction on the electrode surface,[3,4)] the activation energy change consists of the chemical potential change $\Delta\mu$ as well as the interaction energy change ΔE_{int}. In this case, the activation energy E_a increases or decreases by the amount of the change of

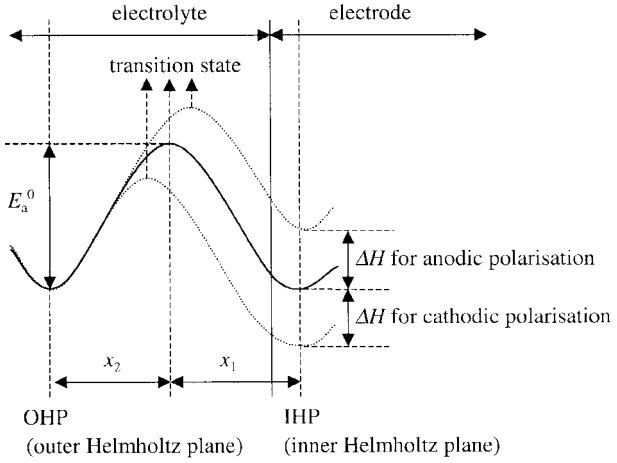

Fig. 1. Schematic diagram of the potential energy curve across the electrolyte/electrode interface for the jumps of atoms or ions from the electrolyte side to the electrode surface side or vice versa. Solid line represents the potential energy curve at open circuit potential (OCP), $\alpha_{anod} = x_1/(x_1 + x_2)$; $\alpha_{cath} = x_2/(x_1 + x_2)$.

ensemble energy as Hamiltonian ΔH multiplied by the symmetry factor α. Fig. 1 shows the schematic diagram of the potential energy curve across the electrolyte/electrode interface for the jumps of atoms or ions from the electrolyte side to the electrode surface side or vice versa in consideration of only the short-range interactions between atoms or ions on the electrode surface.

According to the model, the activation energy E_a during the anodic polarisation is expressed as,[13,14)]

$$E_a = E_a^0 - \alpha_{anod}\Delta H \quad \text{for the anodic reaction} \tag{7}$$

$$E_a = E_a^0 + (1 - \alpha_{anod})\Delta H \quad \text{for the cathodic reaction} \tag{8}$$

where α_{anod} is the symmetry factor for the anodic reaction, *i.e.* for the jumps of atoms or ions from the electrode side to the electrolyte side, $(1\text{-}\alpha_{anod}) = \alpha_{cath}$. By contrast, the activation energy E_a during the cathodic polarisation is given by,

$$E_a = E_a^0 + (1 - \alpha_{cath})\Delta H \quad \text{for the anodic reaction} \tag{9}$$

$$E_a = E_a^0 - \alpha_{cath}\Delta H \quad \text{for the cathodic reaction} \tag{10}$$

where α_{cath} is the symmetry factor for the cathodic reaction, *i.e.* for the jumps of atoms or ions from the electrolyte side to the electrode side, $(1\text{-}\alpha_{cath}) = \alpha_{anod}$.

2.3. Kinetic Monte Carlo procedure for diffusion process

The essential basis in statistical mechanics for the theoretical study on kinetics of diffusion process is the random walk approach. The random walk simulation for diffusion process is performed in the canonical ensemble (CE) where all the microstates have the same volume *V*, the same temperature *T* and the same number of atoms or ions *N* with each other.

The kinetic Monte Carlo procedures for diffusion process with the spin-exchange dynamics[15)] are described as follows:
(i) Establish an initial configuration of the system,
(ii) Select one atom or ion in the system at random,
(iii) Make a random trial jump of the atom or ion to one of its nearest neighbour sites,
(iv) If the nearest neighbour site is occupied, the trial jump of the atom or ion is rejected,
(v) If the nearest neighbour site is empty, W_{tr} is calculated from Eqs. (4) and (6),
(vi) If W_{tr} is greater in value than a random number generated between 0 and 1, the trial jump is accepted; otherwise, the trial jump is rejected, and then repeat the steps (ii) through (vi) under the periodic boundary condition.[11,15)] Monitoring the position of each atom or ion in the system jumping across the periodic boundary by recording the direction and the frequency of the encounter between either atom or ion and the periodic boundary to effectively circumvent the limitation of the finite size.[11,15)]

If the jump direction of atoms or ions randomly diffusing through the system is independent of the previous jump direction, the component diffusivity D_K is simply obtained from the mean square displacement of atoms or ions,

$$D_K = \frac{1}{2dt}\langle \Delta r^2 \rangle = \frac{1}{2dtN}\sum_i^N \Delta r_i^2 \tag{11}$$

where d is the dimension of the system; $<\Delta r^2>$, the mean square displacement per atom or ion at t MCS, and Δr_i^2 represents the square displacement of atom or ion i at t MCS. Here, D_K is a measure of the random motion of atoms or ions, and is thus simply proportional to the mobility of the species in question. This diffusion coefficient obeys the Nernst-Einstein equation regardless of whether the system is ideal or non-ideal solution.

The chemical diffusivity $\tilde{D}$ is expressed as the combination of the thermodynamic enhancement factor W and the component diffusivity D_K in the Kubo-Green formula,[15,16)]

$$\tilde{D} = WD_K \tag{12}$$

which is the well-known Darken equation. In Eq. (12), W is obtained from the fluctuation of N at constant V and T in the grandcanonical ensemble (GCE),

$$W = \left[\frac{\partial(\mu/k_BT)}{\partial \ln \delta}\right]_{V,T} \tag{13}$$

$$= \frac{\delta}{k_BT}\left(\frac{\partial \mu}{\partial \delta}\right)_{V,T} = \frac{\langle N\rangle}{k_BT}\left(\frac{\partial \mu}{\partial N}\right)_{V,T} = \frac{\langle N\rangle}{Var(N)} = \frac{\langle N\rangle}{\langle N^2\rangle - \langle N\rangle^2} \tag{14}$$

where δ is the concentration of atoms or ions; $<N>$ and $<N^2>$, the mean values of N and N^2, respectively, and $Var(N)$ represents the variance of N.

3. Electrochemical Reaction Kinetics by Kinetic Monte Carlo Method

In the field of electrochemistry, the current response measured during the potential step (*i.e.* potentiostatic current transient technique or chronoamperometry) or during the potential scan (*i.e.* cyclic voltammetry or linear sweep voltammetry) has been analysed to understand kinetics of the electrochemical reactions. In this section, we introduce the kinetic Monte Carlo procedures to calculate the current responses during both potential step and scan under the assumption that the charge-transfer reaction occurs so rapid that diffusion process is the rate-controlling step of the electrochemical reactions. Let us consider an intercalation electrode with planar symmetry immersed into an electrolyte containing alkali ions that can be intercalated into the electrode without interactions, *i.e.* a Langmuir gas. In addition, assume that the charge-transfer reaction occurs at the electrode surface, and the intercalated alkali ions diffuse through the electrode and then accumulate at the end of the electrode as an impermeable boundary.

3.1. Potentiostatic current transient by kinetic Monte Carlo method

In the case of the pontetiostatic current transient technique, the current response is measured with time after an abrupt potential jump or drop from an initial electrode potential to an

applied constant potential. Under the diffusion-controlled constraint, the concentration of ions at the electrode surface is maintained constant as the concentration corresponding to the applied potential during the potential jump or drop, which is determined from the relationship between the electrode potential and the concentration of ions (see the inset in Fig. 2).

In the kinetic Monte Carlo procedure, the above boundary condition (B.C.) at the electrode surface is written as

$$P(\{c\}, t)|_{x=0} = \delta_s, \quad \text{for } t > 0 \tag{15}$$

where δ_s is the surface concentration of ions, and x represents the distance from the surface to the end of the electrode. On the other hand, the impermeable B.C. at the end of the electrode is given by

$$\left.\frac{\partial P(\{c\}, t)}{\partial t}\right|_{x=L} = -J(\{c\}, t)|_{x=L} = 0, \quad \text{for } t > 0 \tag{16}$$

where L is the thickness of the electrode.

By using Eqs. (2), (3), (4) with Eqs. (6), (15) and (16), the flux of ions at the electrode surface and those fluxes at any of the inside electrode can be calculated as a function of MCS time. Here, the plot of the flux of ions at the electrode surface against MCS time corresponds to the current transient. The flux of ions and the MCS time were reduced by the total number of sites on the electrode surface side and the square of the total number of sites in the thickness direction being perpendicular to the electrode surface, respectively.

Fig. 2 gives on a logarithmic scale the anodic current transient theoretically calculated under the diffusion-controlled constraint by jumping the initial electrode potential -0.2 V to the anodic potential 0.2 V. The current transient theoretically calculated exhibited a linear relationship between logarithmic flux and logarithmic time with a slope of -0.5, followed by an exponential decay. The transition time t_T indicated by open circle means the time at which the current transient shows a transition from the semi-infinite diffusion process (*i.e.* the Cottrell behaviour) to the finite-length diffusion process.[17,18)]

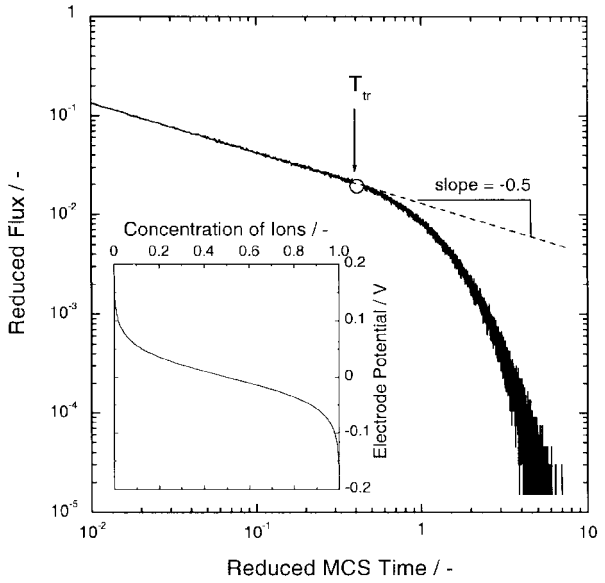

Fig. 2. Anodic current transient theoretically calculated under the diffusion-controlled constraint by jumping the initial electrode potential −0.2 V to the anodic potential 0.2 V. The relationship between the electrode potential and the concentration of ions is presented as the inset in figure.

3.2. Linear sweep voltammogram by kinetic Monte Carlo method

In the case of the linear sweep voltammetry, the current response is obtained by scanning the applied potential from an initial electrode potential to a final potential at a scan rate v. Under the diffusion-controlled constraint, the variation in the surface concentration of ions with time follows the change in the concentration of ions with the quotient of the

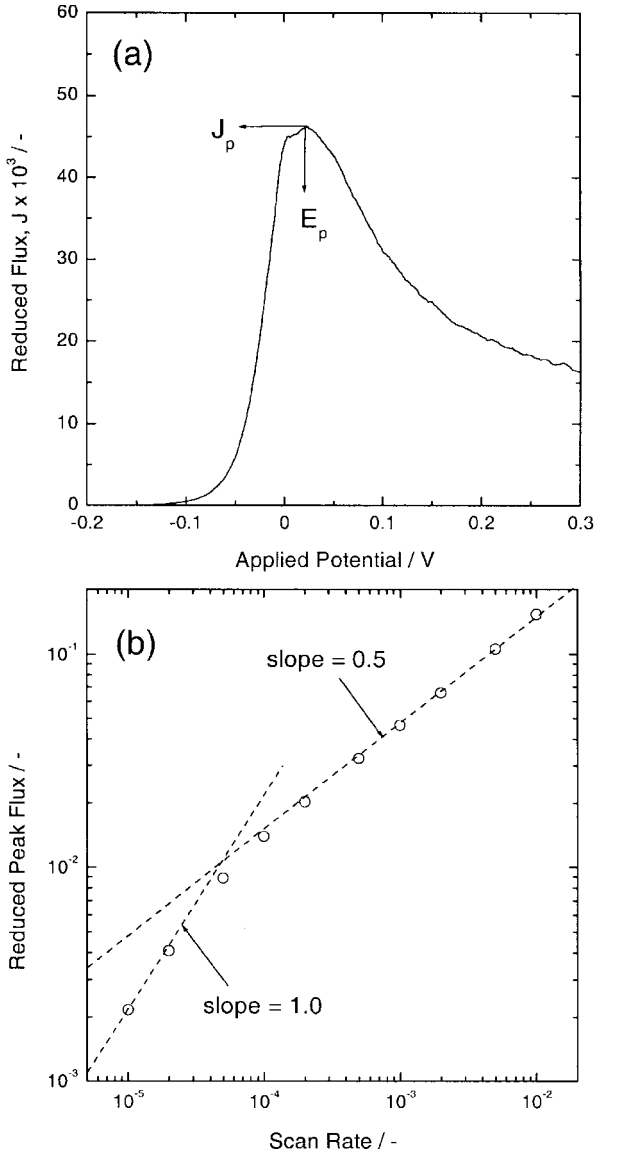

Fig. 3. (a) Linear sweep voltammogram theoretically calculated under the diffusion-controlled constraint by scanning the applied potential from −0.2 to 0.3 V with the scan rate of $v = 1 \times 10^{-3}$, and (b) the reduced peak flux J_p theoretically calculated at various scan rates v.

applied potential divided by the potential scan rate, according to the relationship between the electrode potential and the concentration of ions (see the inset in Fig. 2).

According to the Nernst equation,[13] the above B.C. at the electrode surface in the kinetic Monte Carlo procedure is written as,

$$P(\{c\},t)|_{x=0} = \delta_s(t) = \exp\left[\frac{zF}{RT}(E_i + vt)\right], \text{ for } t > 0 \quad (17)$$

where z is the charge valence; F, the Faraday constant; R, the gas constant; E_i, the initial electrode potential, and v represents the scan rate given by (dE/dt). In Eq. (17), v has a positive value for the anodic scan, while v has a negative value for the cathodic scan. By using Eqs. (2), (3) and (4) with Eqs. (6), (16) and (17), the flux of ions at the electrode surface and those fluxes at any of the inside electrode can be calculated as a function of MCS time. Here, the plot of the flux of ions at the electrode surface against the applied potential corresponds to the linear sweep voltammogram.

Fig. 3(a) depicts the linear sweep voltammogram theoretically calculated under the diffusion-controlled constraint by scanning the applied potential from -0.2 to 0.3 V with the scan rate of $v = 1 \times 10^{-3}$. The linear sweep voltammogram theoretically calculated showed one reduced peak flux J_p at the peak potential E_p. The reduced peak flux J_p was calculated at various scan rates as given in Fig. 3(b).

In Fig. 3(b), log J_p was clearly proportional to log v with a slope of 0.5 at the high scan rates (*i.e.* Randles-Sevcik relation) and with a slope of 1.0 at the low scan rates, as well-established for the diffusion-controlled transport of atoms or ions under the impermeable boundary condition on one side of the electrode. The former proportionality on a logarithmic scale is attributed to the semi-infinite diffusion process, whereas the latter proportionality does to the finite-length diffusion process.[19]

4. Application of kinetic Monte Carlo Method to Electrochemical Lithium Intercalation into $LiMn_2O_4$

4.1. Component and chemical diffusivity of lithium ions

In this section, we apply the kinetic Monte Carlo method to investigate kinetics of the electrochemical lithium intercalation into the $LiMn_2O_4$ electrode involving the disorder to order phase transition,[9,10] one of the well-known intercalation compounds. For the kinetic Monte Carlo simulation, we employed the two sub-lattice model of the $LiMn_2O_4$ electrode well-established in the previous works.[9,10,20]

In consideration of the first- and second-nearest interactions between lithium ions in the $LiMn_2O_4$ electrode, Hamiltonian H of the lattice is defined as[9,10]

$$H = J_1 \sum_{ij} c_i c_j + J_2 \sum_{ik} c_i c_k - (\varepsilon + \mu) \sum_i c_i \quad (18)$$

where J_1 and J_2 are the effective pairwise interaction parameters for the first- and second-nearest neighbouring lithium ions, respectively; ε, the effective binding energy between lithium ion and manganese oxide matrix; μ, the chemical potential of lithium ion; c_i, the local occupation number of the site i, and c_j and c_k represent the local occupation numbers of the first- and second-nearest neighbour sites, respectively: c_i, c_j or $c_k = 1$ if the site is occupied by lithium ion, and c_i, c_j or $c_k = 0$ otherwise. In this article, the values of the effective interaction parameters were similarly taken as $J_1 = 37.5$ meV, $J_2 = -4.0$ meV and $\varepsilon = 4.12$ eV which allowed us to successfully approximate the thermodynamic properties of the $LiMn_2O_4$ electrode.[9,10,20]

Fig. 4 presents on a logarithmic scale the component diffusivity D_K and the chemical diffusivity $\tilde{D}$ of lithium ions along with the thermodynamic enhancement factor W, theoretically calculated as a function of lithium content $(1-\delta)$ in $Li_{1-\delta}Mn_2O_4$ at $T = 298$ K from Eqs. (11), (12), (13) and (14). In order to analyse the dependence of $\tilde{D}$ on $(1-\delta)$, we compared the contribution of D_K to $\tilde{D}$ with that contribution of W. Below the transition point $(1-\delta)_{tr1}$ at which the transition of the disordered lithium-poor phase to the ordered phase occurs,[10] D_K decreased exponentially with $(1-\delta)$ while W increased linearly. Therefore, $\tilde{D}$, which is mainly governed in value by D_K below $(1-\delta)_{tr1}$, decreased with $(1-\delta)$ due to the decrease of the available vacant sites for diffusion.

Above the transition point $(1-\delta)_{tr2}$ at which the transition of the ordered phase to the lithium-rich phase occurs,[10] $\tilde{D}$ increased with $(1-\delta)$, indicating that $\tilde{D}$ is predominantly controlled in value by W owing to the suppressed fluctuation in N. On the other hand, in the ordered phase region between $(1-\delta)_{tr1}$ and $(1-\delta)_{tr2}$, $\tilde{D}$ held nearly constant value due to the counterbalancing effects of D_K and W. In our recent work,[10] the results theoretically calculated were compared with those

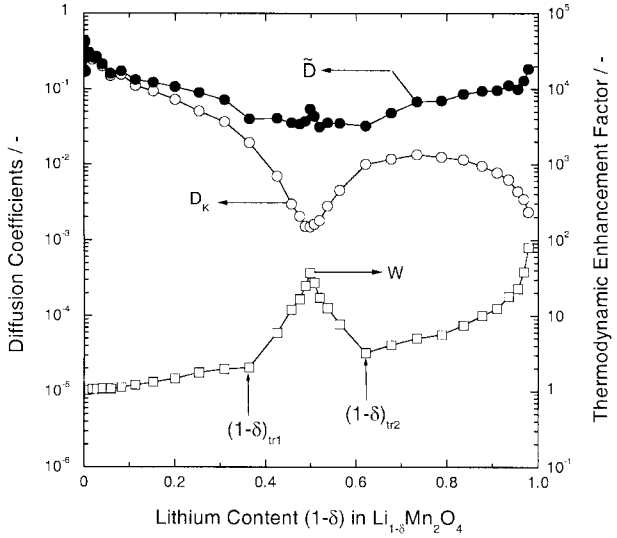

Fig. 4. Plots of the component diffusivity D_K and the chemical diffusivity $\tilde{D}$ along with the thermodynamic enhancement factor W, theoretically calculated as a function of lithium content $(1-\delta)$ in the $Li_{1-\delta}Mn_2O_4$ electrode at $T = 298$ K. $(1-\delta)_{tr1}$ means the transition point of the disordered lithium-poor phase to the ordered phase, and $(1-\delta)_{tr2}$ represents the transition point of the ordered phase to the disordered lithium-rich phase.[10]

results experimentally measured, and then the effects of such structural defects as the excess lithium ions and oxygen vacancies on $\tilde{D}$, D_K and W were also discussed.

4.2. Potentiostatic current transient and linear sweep voltammogram

Recently, in our works[21-26] on lithium transport through the transition metal oxides, it was found that the potentiostatic current transient and the cyclic voltammogram experimentally measured never follow the diffusion-controlled behaviours, *i.e.* the Cottrell equation and the Randles-Sevcik equation, respectively. From the numerical analyses of the current transient and the cyclic voltammogram, it was suggested that lithium transport through the oxides is controlled by the cell-impedance rather than diffusion of lithium ions in the oxides. In those works, the cell-impedance means the total internal cell resistance, major sources of which may be the bulk electrolyte, the electrolyte/electrode interface, and the bulk electrode.

According to the cell-impedance-controlled model, the current I is crucially determined by the quotient of the potential difference ΔE between the equilibrium electrode potential E_{eq} and the applied potential E_{app} divided by the cell-impedance R_{cell},[21-26]

$$I = (E_{app} - E_{eq})/R_{cell} = \Delta E/R_{cell} \quad (19)$$

In the kinetic Monte Carlo procedure, therefore, the flux of lithium ions at the electrolyte/electrode interface is calculated as a function of MCS time by using W_{tr} given as,

$$W_{tr} = f|E_{app} - E_{eq}| = f|\Delta E| \quad (20)$$

where f is the proportionality (conversion) factor, and $|E_{app}\text{-}E_{eq}|$ represents the potential difference ΔE between E_{eq} and E_{app} in absolute value. In Eq. (20), W_{tr} is again proportional to the quotient of ΔE in absolute value divided by R_{cell} as follows,

$$W_{tr} \propto \frac{|\Delta E|}{R_{cell}} \quad (21)$$

This means that the conversion factor f is inversely proportional to R_{cell}.

Fig. 5 gives on a logarithmic scale the anodic current transients, theoretically calculated by the kinetic Monte Carlo method under the cell-impedance-controlled constraint with the conversion factors $f = 0.1$ and 0.2 by jumping the electrode potential 3.90 $V_{Li/Li+}$ to the applied potential 4.30 $V_{Li/Li+}$. The current transient theoretically calculated ran with the slope of logarithmic reduced flux with logarithmic time flatter than -0.5 in the early stage, and then did in the upward concave shape in the time interval between the first inflection point t_{T1} and the second inflection point t_{T2}, finally followed by an exponential decay. The reduced flux J in the early stage increased, and t_{T1} and t_{T2} were shortened with increasing f (*i.e.* decreasing R_{cell}). The current transient theoretically calculated under the cell-impedance-controlled constraint well coincided in shape with the result experimentally measured.[25,26]

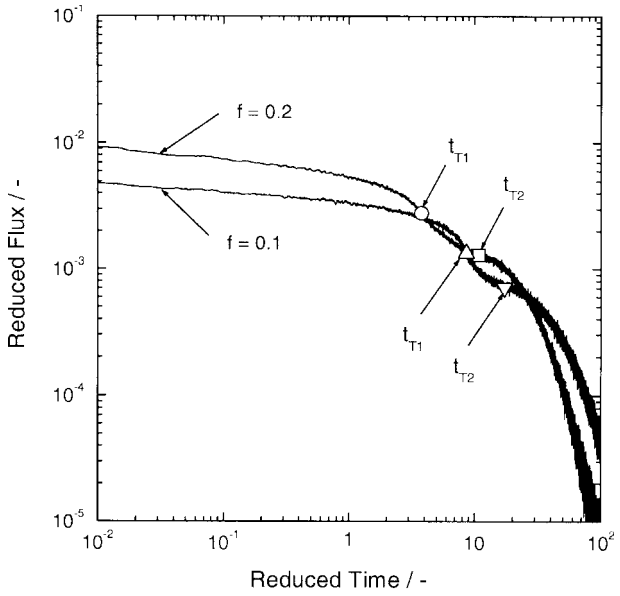

Fig. 5. Anodic current transients theoretically calculated under the cell-impedance-controlled constraint with the conversion factors f = 0.1 and 0.2 by jumping the electrode potential 3.90 $V_{Li/Li+}$ to the applied potential 4.30 $V_{Li/Li+}$.

Fig. 6(a) demonstrates the linear sweep voltammogram, theoretically calculated by the kinetic Monte Carlo method under the cell-impedance-controlled constraint with $f = 0.2$ by scanning the applied potential from 3.80 to 4.50 $V_{Li/Li+}$ with the scan rate of $v = 1\times10^{-3}$. The linear sweep voltammogram theoretically calculated exhibited two reduced peak fluxes J_{p1} and J_{p2} at the peak potentials E_{p1} and E_{p2}, respectively. The linear sweep voltammogram theoretically calculated was well consistent in shape with the result experimentally measured.[26] The reduced peak fluxes J_{p1} and J_{p2} which were determined from the linear sweep voltammograms calculated at various scan rates v and conversion factors f are shown in Fig. 6(b).

In Fig. 6(b), the dependence of logarithmic reduced peak fluxes on logarithmic scan rates did not follow the Randles-Sevcik relation at the high scan rates. The first reduced peak flux J_{p1} and the second reduced peak flux J_{p2}, calculated under the cell-impedance-controlled constraint with $f = 0.1$, were linearly proportional to v to the power of 0.54 ($J_{p1} \propto v^{0.54}$) and 0.58 ($J_{p2} \propto v^{0.58}$) at the high scan rates. The slopes of log J_{p1} and log J_{p2} *vs.* log v plots calculated with $f = 0.2$ were determined to be 0.57 ($J_{p1} \propto v^{0.57}$) and 0.61 ($J_{p2} \propto v^{0.61}$), respectively, indicating that those slopes became steeper with increasing f (*i.e.* decreasing R_{cell}). The dependence of the peak flux on the scan rate theoretically calculated by the kinetic Monte Carlo method under the cell-impedance-controlled constraint well coincided with the results experimentally measured,[26] indicating that lithium transport through the $LiMn_2O_4$ electrode is not underlain by the diffusion-controlled constraint but by the cell-impedance-controlled constraint.

From the results theoretically calculated in the case of the $LiMn_2O_4$ electrode, one can readily find that the kinetic

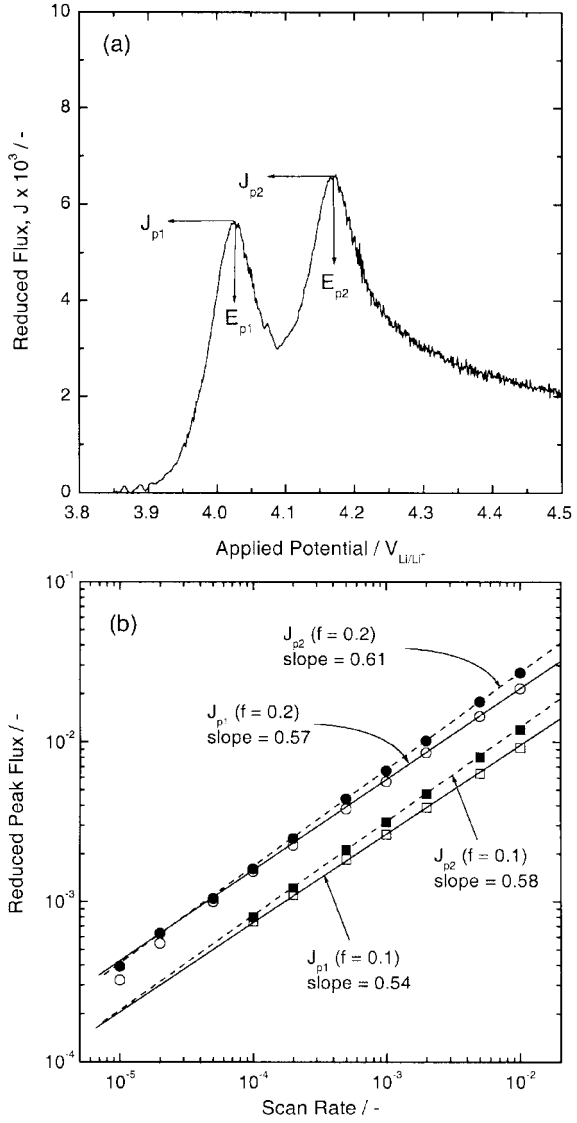

Fig. 6. (a) Linear sweep voltammogram theoretically calculated under the cell-impedance-controlled constraint with $f = 0.2$ by scanning the applied potential from 3.80 to 4.50 $V_{Li/Li+}$ with the scan rate of $v = 1 \times 10^{-3}$, and (b) the reduced peak fluxes J_{p1} and J_{p2} theoretically calculated at various scan rates v and conversion factors f.

Monte Carlo method based upon the transition state theory is much relevant to theoretically investigate kinetics of the lithium intercalation in the field of electrochemistry.

5. Conclusions

The present article first reviewed the fundamentals of the kinetic Monte Carlo methods and the transition state theory, and then applied the kinetic Monte Carlo methods based upon the transition state theory to evaluate diffusion kinetics. The kinetic Monte Carlo methods were employed to analyse the current responses during the potential step and scan under the simple diffusion-controlled constraint. In addition, the kinetic Monte Carlo simulation was executed to analyse the current transient and the linear sweep voltammogram of the $LiMn_2O_4$ electrode, one of the intercalation compounds, under the cell-impedance-controlled constraint. From the results theoretically calculated, it was confirmed that the kinetic Monte Carlo method based upon the transition state theory with appropriate boundary conditions is strongly applicable to analyse kinetics of the electrochemical lithium intercalation.

Acknowledgement

This work was partly supported by the Brain Korea 21 project.

References

1. D. T. Gillespie, *J. Comp. Phys.*, **22**, 403 (1976).
2. D. T. Gillespie, *J. Phys. Chem.*, **81**, 2340 (1977).
3. J. J. Lukkien, J. P. L. Segers, P. A. J. Hilbers, R. J. Gelten and A. P. J. Jansen, *Phys. Rev. E*, **58**, 2598 (1998).
4. S. J. Mitchell, G. Brown and P. A. Rikvold, *Surf. Sci.*, **471**, 125 (2001).
5. C. Uebing and R. Gomer, *J. Chem. Phys.*, **95**, 7626 (1991).
6. C. Uebing and R. Gomer, *J. Chem. Phys.*, **95**, 7636 (1991).
7. C. Uebing and R. Gomer, *J. Chem. Phys.*, **95**, 7641 (1991).
8. C. Uebing and R. Gomer, *J. Chem. Phys.*, **95**, 7648 (1991).
9. R. Darling and J. Newman, *J. Electrochem. Soc.*, **146**, 3765 (1999).
10. S. -W. Kim and S. -I. Pyun, *Electrochim. Acta*, **46**, 987 (2001).
11. K. W. Kehr and K. Binder, "Simulation of Diffusion in Lattice Gases and Related Kinetic Phenomena", in Applications of the Monte Carlo Method in Statistical Physics, ed. by K. Binder, 181-221, Springer-Verlg, New York (1984).
12. R. Nassif, Y. Boughaleb, A. Hekkouri, J. F. Gouyet and M. Kolb, *Eur. Phys. J. B*, **1**, 453 (1998).
13. A. J. Bard and L. R. Faulkner, "Electrochemical Methods: Fundamentals and Applications", 86-118, Wiley, New York (1980).
14. S. -I. Pyun, "Outlines of Electrochemistry of Materials", 226-286, Sigma press, Seoul (2001).
15. K. Binder and D. W. Heermann, "Monte Carlo Simulation in Statistical Physics - An Introduction", Springer-Verlag, New York (1997).
16. R. Gomer, *Rep. Prog. Phys.*, **53**, 917 (1990).
17. C. J. Wen, B. A. Boukamp, R. A. Huggins and W. Weppner, *J. Electrochem. Soc.*, **126**, 2258 (1979).
18. A. J. Vaccaro, T. Palanisamy, R. L. Kerr and J. T. Maloy, *J. Electrochem. Soc.*, **129**, 682 (1982).
19. K. Aoki, K. Tokuda and H. Matsuda, *J. Electroanal. Chem.*, **146**, 417 (1983).
20. Y. Gao, J. N. Reimers and J. R. Dahn, *Phys. Rev. B*, **54**, 3878 (1996).
21. H. -C. Shin and S. -I. Pyun, *Electrochim. Acta*, **45**, 489 (1999).
22. H. -C. Shin and S. -I. Pyun, *Electrochim. Acta*, **46**, 2477 (2001).
23. H. -C. Shin, S. -I. Pyun, S. -W. Kim and M. -H. Lee, *Electrochim. Acta*, **46**, 897 (2001).
24. M. -H. Lee, S. -I. Pyun and H. -C. Shin, *Solid State Ionics*, **140**, 35 (2001).
25. S. -I. Pyun and S. -W. Kim, *J. Power Sources*, **97-98**, 371 (2001).
26. S. -W. Kim and S. -I. Pyun, *Electrochim. Acta*, **47**, 2843 (2002).